SUPPLEMENTARY INFORMATION

Tudor domain ERI-5 tethers an RNA-dependent RNA polymerase to DCR-1 to potentiate endo-RNAi

Caroline Thivierge[1,2,6], Neetha Makil[1,2,6], Mathieu Flamand[1,2], Jessica J. Vasale[3], Craig C. Mello[3,4], James Wohlschlegel[5], Darryl Conte Jr.[3] & Thomas F. Duchaine[1,2]

[1]Department of Biochemistry, McGill University, Montreal, Quebec, H3G 1Y6, Canada. [2]Goodman Cancer Center, McGill University, Montreal, Quebec, H3G 1Y6, Canada. [3]Program in Molecular Medicine, University of Massachusetts Medical School, 373 Plantation Street, Suite 219, Worcester, Massachusetts, 01605, USA. [4]Howard Hughes Medical Institute, University of Massachusetts Medical School, 373 Plantation Street, Suite 219, Worcester, Massachusetts 01605, USA. [5]Department of Biological Chemistry, David Geffen School of Medicine, University of California Los Angeles, Los Angeles, California 90095, USA. [6]These authors contributed equally. Correspondence should be addressed to T.F.D. (thomas.duchaine@mcgill.ca).

Supplementary Figure-1

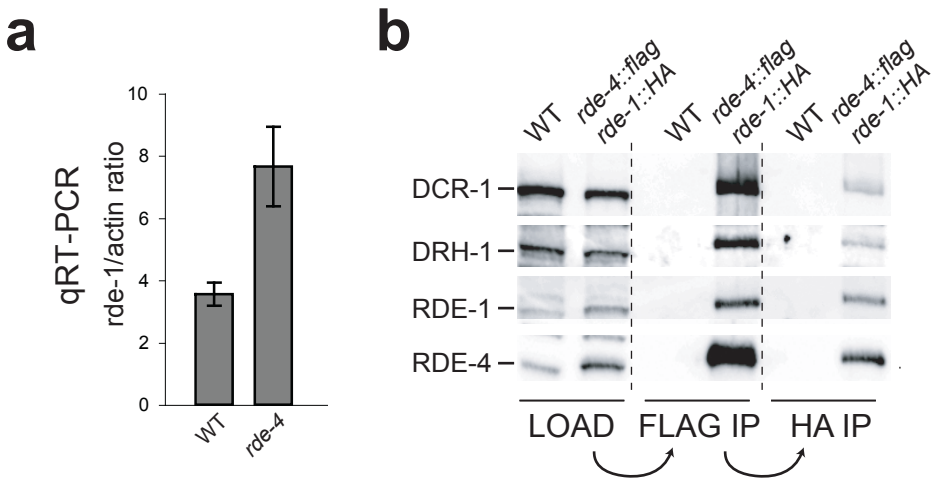

Supplementary Figure 1.

Distinct DCR-1 complexes initiate endo- and exoRNAi.

(**a**) Expression of *rde-1* mRNA by qRT-PCR analysis. Total RNA from wild-type (WT) and *rde-4* mutant embryos were used. *Rde-1* mRNA levels were normalized to an actin control. Results are presented as the mean from triplicate samples and error bars represent sd.

(**b**) FLAG, HA sequential IP in WT and rde-4::flag; rde-1::HA double mutant embryos. DCR-1, DRH-1, RDE-1 and RDE-4 proteins were detected by western blot.

Supplementary Figure-2

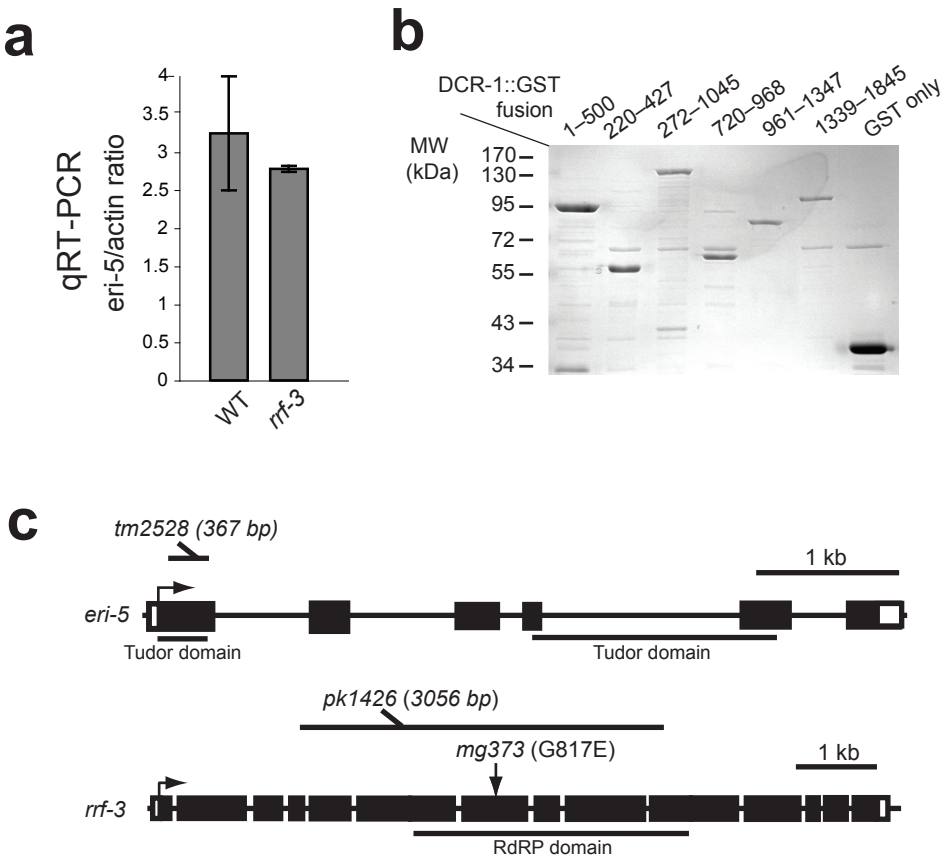

Supplementary Figure 2.

ERI-5 recruits an RdRP module to DCR-1 N-terminus.

(**a**) Shown is the expression profile of *eri-5* mRNA by qRT-PCR analysis. Total RNA from WT and *rrf-3* (*pk1426*) mutant embryos were used. *Eri-5* mRNA levels were normalized to an actin control. Results are presented as the mean from triplicate samples and error bars represent standard deviation.

(**b**) Coomassie Blue gel staining showing purified DCR-1-GST fusion proteins.

(**c**) Schematic representation of *eri-5* (*tm2528*) and *rrf-3* (*pk1426*) deletion mutants and *rrf-3* (*mg373*) point mutant.

Supplementary Figure-3

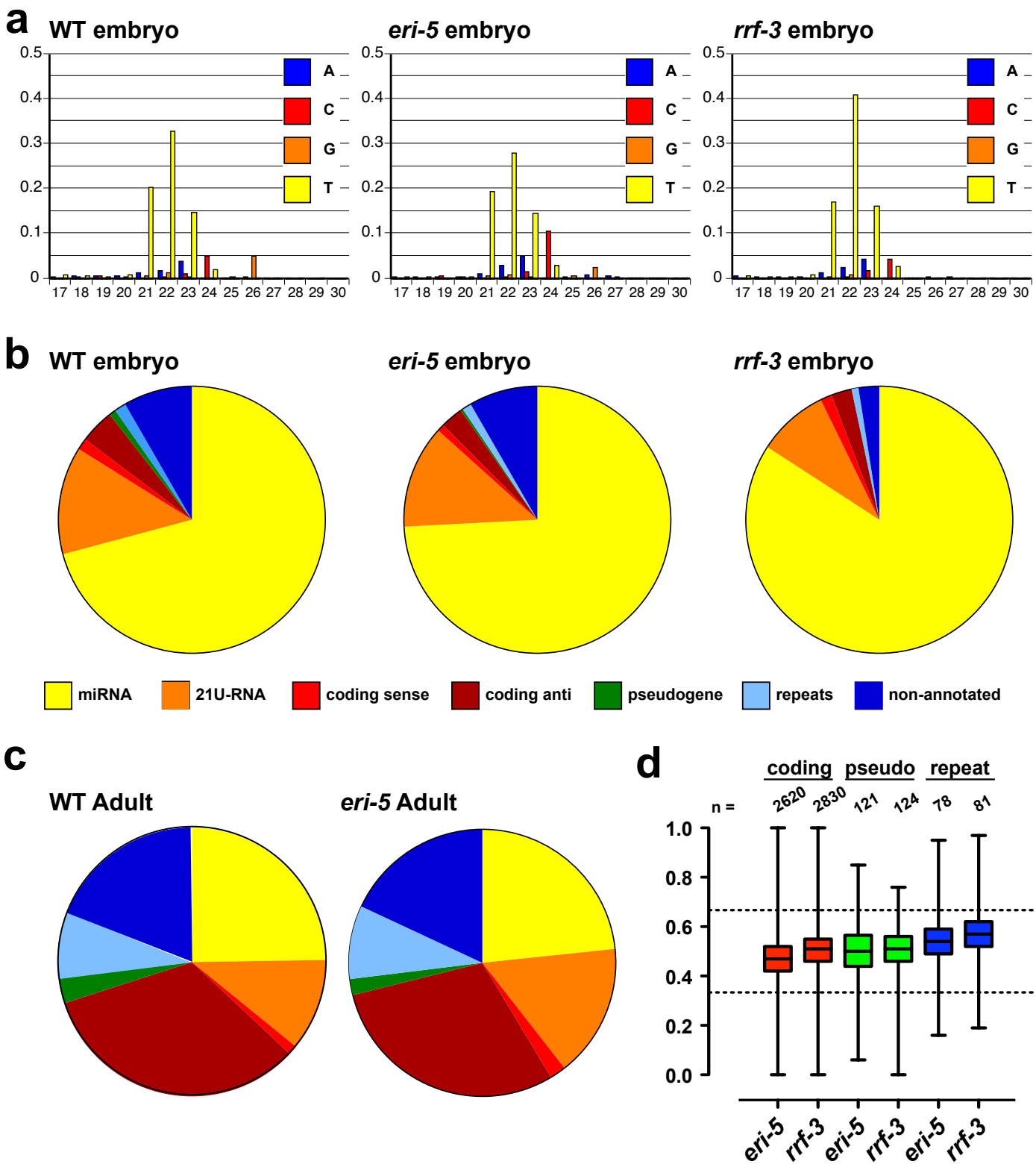

Supplementary Figure 3.

Deep sequencing analysis of *eri-5* mutant.

(**a**) Length and first nucleotide distribution of small RNAs cloned from wild-type (WT), *eri-5* and *rrf-3* embryos. The y-axis represents the fraction of total normalized reads. The x-axis represents the read length in nucleotides (nt). Note that 26nt reads starting with a 5'G represent ~5% in WT, ~2.5% in *eri-5*, and ~0.05% in *rrf-3*.

(**b**) Pie charts showing the distribution of genome matching reads in the small RNA libraries prepared from WT, *eri-5* and *rrf-3* mutant embryos.

(**c**) Pie charts showing the distribution of genome matching 22G-RNA reads in the small RNA libraries prepared from WT and *eri-5* adults. The WT sample was previously published (Gu et al., 2009).

(**d**) Box and whisker plots showing 22G-RNAs that are not downstream of the ERI endo-RNAi pathway are unaffected in *eri-5* and *rrf-3* mutants. These loci include protein coding genes, pseudogenes and transposons (repeats) as described (Gu et al., 2009).

See legend of Figure 3 for description of box and whisker plots. The number of loci used to generate each box-and-whisker plot is indicated above each plot and the data are provided in Supplementary Table 2.

Supplementary Figure-4

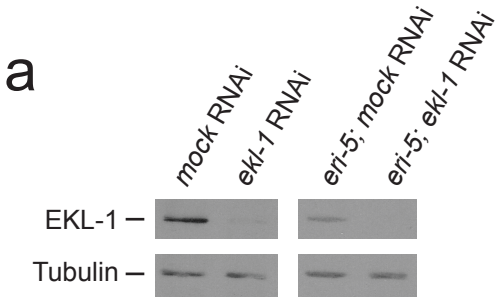

Supplementary Figure 4.

ERI-5 potentiates ERI endoRNAi small RNA biogenesis.

(a) *Ekl-1* RNAi efficiency in *C.elegans* mock RNAi (*sel-1*), *ekl-1* RNAi, *eri-5*; mock RNAi (*sel-1*) and *eri-5*; *ekl-1* RNAi embryos. EKL-1 protein knock-down was determined by western blot and tubulin was used as a loading control.

Supplementary Results:

Coupled stability of the RDE complex components (see Fig. 1b).

Unexpectedly, when *dcr-1-/-* extracts were probed by western blot, neither RDE-1 nor DRH-1 could be detected. Similarly, when *rde-4* extracts were probed, RDE-1 could barely be detected. The reduction in the expression of RDE-1 was not complete, and low levels of RDE-1 expression could still be detected in the *dcr-1-/-* background, but only when enriched from an RDE-4 IP. This coupling in protein expression is likely to occur at the level of protein stability, as the mRNA levels for *rde-1* were in fact increased in the *rde-4* genotype (Supplementary Fig.1a). No RDE-1 interaction with DRH-1 or DCR-1 was detected in the *rde-4* background (Figure 1B DRH-1 and DCR-1 IP panels, *rde-4* lane). The interaction between DRH-1 and DCR-1 remained unaffected in the *rde-1* and *rde-4* backgrounds, and interaction between RDE-1 and RDE-4 could still be detected in the *dcr-1* genotype (which also lacks DRH-1, see below). In addition, RDE-4 could still interact with DCR-1 in the *rde-1* background (Fig. 1b RDE-4, DRH-1 and DCR-1 IP panels, *rde-1, rde-4, dcr-1* lanes). Together, these results indicate that RDE-1 is stabilized and recruited to DCR-1 via its interaction with RDE-4, and independently of DRH-1, but that they assemble within a common complex.

Supplementary Methods:

Real-time PCR For mRNA analysis of *eri-5* and *rde-1*, real-time PCR was performed as described in (Duchaine et al., 2006).

Sequence of primer pairs

qRT-PCR

Eri-5 mRNA:

5′ GCGAAATGGAGTGGAATACAC 3′ and

5′ CGAATCTGCGAGAATTGCAG 3′

Rde-1 mRNA:

5′ GGAATGAGCCAAGATGAAGTC 3′ and

5′ GCATAATGAACCGGAACAGG 3′

actin:

5′ CGTGTTCCCATCCATTGTCG 3′ and

5′ AGTTGGTGACGATACCGTGCTC 3′

***C40A11.10* (26-G) qRT-PCR:**

Universal: 5′ CATGATCAGCTGGGCCAAGA 3′

GSP: 5′ CATGATCAGCTGGGCCAAGACGGAATCTCA 3′

LNA (26-G): 5′ G+CA+AGATGGAAAAG 3′

***X-cluster* qRT-PCR:**

GSP: 5′ CATGATCAGCTGGGCCAAGACTCATACCG 3′

LNA (X): 5′ G+AA+TAGATACGCGG 3′

Cloning

Eri-5 cDNA:

pCalkc:

5′ tttttggatccTGCTCTCGGAGGAGCCCTACG 3′

5′ tttttggatccTCCGCTATCCTTATCGTCGC 3′

pET42 and pET28:

5′ tttttggatccATGCTCTCGGAGGAGCCCTACG 3′

Eri-3 cDNA:

pET28/3XFlag:

5′ CTCGAGTGCAACCCGTTCTTGTAAATAG 3′

5′ CTCGAGTCATTCAATAAACGGGGATTCTGTAC 3′

Ekl-1 cDNA:

pCalkc:

5′ agatct TG ATT GCG GTT GGA CTC CG 3′

5′ agatct ATT TGG CCA TTC GAT TGG CTC 3′

Starfire probe sequences:

C40A11.10:

5′ CGG AAT CTC AAA CTT TTC CAT CTT GC/StarFire 3′

X-cluster: (mix of these two probes)

5′ CTC ATA CCG CGT ATC TAT TC/StarFire 3′

5′ CGC GTA TCT ATT CAA TTG AAT/StarFire 3′